Scientific paper

MnO_2 Submicroparticles from Chinese Brush and Their Application in Treatment of Methylene Blue Contaminated Wastewater

Qi Wang,[1,*] Chunlei Ma,[1] Wanjun Li,[1] Meng Fan,[2] Songdong Li[1] and Lihua Ma[3,*]

[1] *Chemistry & Chemical Engineering Department, Taiyuan Institute of Technology, Taiyuan 030008, China.*

[2] *Research Center for Eco-Environmental Sciences in Shanxi, Taiyuan 030009, China*

[3] *Department of Chemistry, University of Houston at Clear Lake, Houston 77058, USA*

** Corresponding author: E-mail: wangqitit@163.com; mal@uhcl.edu.*

Received: 30-07-2016

Abstract

Eggshell membrane (ESM) is selected as biotemplate to prepare MnO_2 submicroparticles (SMPs) using Chinese Brush with sodium hydroxide solution. The size with average 710 nm of the obtained materials is in good consistency with the microsructured biotemplate. An efficient and convenient absorbent for methylene blue (MB) is developed. The removal efficiency could reach up to 93% in 35 min under room temperature without pH adjusting owing to the excellent adsorption from ESM itself and hydroxyl group formed on the surface of MnO_2 crystal in the aqueous solution. Materials on the membrane can be separated from the wastewater simply to avoid the secondary pollution caused by the leak of material. This interesting approach to MnO_2 SMPs and facile operation for MB adsorption could open a new path to the submicro-materials based wastewater treatment.

Keywords: MnO_2 particles, biotemplate, eggshell membrane, methylene blue

1. Introduction

Synthesis of inorganic materials by biotemplating as a burgeoning technique has emerged for years in a wide variety of research fields.[1] The use of biotemplate makes the synthetic procedure simple and product controllable taking advantage of the nature of their own. Biotemplates like organisms (butterfly wing,[2] hair,[3] wood fiber[4,5] and pollen[6]), microorganisms (bacteria,[7,8] fungus,[9,10] and viruses[11]) and biological macromolecules (DNA,[12–14] RNA,[15] proteins,[16–19] and polysaccharides[20]) were reported to prepare inorganic materials. Among these templates, proteins have gained more popularity by researchers,[21] ranging from ferritin,[22–25] bovine serum albumin (BSA)[26–31] to collagen[32–34]. However, proteins from natural extracted or artificial synthetic are difficult to obtain and thus cost a lot. This could be a pivotal limitation for the large-scale synthesis and practical application of the biotemplated materials.

Eggshell membrane (ESM) is a kind of biomaterial with great imperative though it is generally considered as a domestic waste.[35] This microscopic biopolymeric fibrous net is composed mainly of proteins (80–85%), 10% of which are collagens and 70–75% are other proteins and glycoproteins.[36] Due to the unique structure and property, ESM has been utilized as a biotemplate for synthesis of inorganic materials. Novel metal materials such as gold nanoparticles, silver nanoparticles, macroporous silver network, Pt-Ag/polymers, have been constructed through ESM templating.[37–40] On the other hand, sulfide,[41] selenide,[42] oxidide[43,44] have been synthesized using ESM as a template. Besides, other kinds of material based on ESM have been studied.[45–47]

As a kind of inorganic nanomaterials, MnO_2 have drawn much attention because of their flexible structures and unique properties and have been applied to catalysis, ion exchange, supercapacitors, molecule adsorption, biosensors and so on.[48] One of the recent applications has fo-

cused on the MnO_2 based micromotors.[49–52] And micromotors containing manganese oxide and noble metal or graphene have also been studied.[53–55]

In this work, by consideration of its special microstructure, abundant component of protein, we choose ESM as the biotemplate to help synthesize MnO_2. Most important of all, ESM could be obtained expediently and free of charge. Furthermore, on the basis of the interaction between protein and metal ions, a novel and interesting procedure with Chinese Brush to grow MnO_2 submicroparticles (MnO_2 SMPs) on ESM is developed. As reported by Furuichi et al, hydroxyl groups could be formed on the surface of MnO_2 in aqueous solutions.[56] Cao et al confirmed that the hydroxyl groups were involved in the adsorption.[48] Therefore, combining the adsorption capacities of both ESM itself[57] and hydroxyl groups formed on the surface of MnO_2 in the aqueous media, these accessible MnO_2 SMPs are applied successfully to the treatment of methylene blue (MB) wastewater.

2. Experimental

2. 1. Reagents and Apparatus

Deionized water with conductivity of 18.2 mΩ cm^{-1} was used in this experiment from a water purification system (ULUPURE, Chengdu, China). Manganese acetate ($MnAc_2$, M_w = 245.09, AR) and methylene blue (MB) were purchased from Kemiou Chemical Co. Ltd. (Tianjin, China). Sodium hydroxide (NaOH, AR) and all the other reagents were at least of analytical grade. Eggshell was obtained from Hongye student mess hall of Taiyuan Institute of Technology, and eggshell membrane was peeled off from the shell carefully. Diluents with different pH values were prepared by titrating with 0.1 mol L^{-1} sodium hydroxide or hydrochloric acid solution to the required pH values.

Scanning electron microscopy (SEM) of ESM and MnO_2 SMPs were carried out on a Quanta 200 FEG scanning electron microscope. The size distribution of as-prepared nanomaterial was performed at a laser particle sizer (Malvern Nano-ZS90). The X-ray photoelectron spectroscopy (XPS) was measured with an AXIS ULTRA DLD electron spectrometer (Kratos) using monochromatic Al Kα radiation for analysis of the surface composition and chemical states of the product. Thermogravimetry (TG) measurement was carried out in air at a heating rate of 10 °C min^{-1} on a Rigaku TG thermal analyzer (Rigaku Co., Japan). The UV-vis absorption spectra were recorded on a TU-1901 UV-vis spectrophotometer (Puxi, China).

2. 2. Synthesis of MnO_2 SMPs

MnO_2 SMPs in this experiment were synthesized through a simple and interesting method. In a typical process, eggshell membrane (ESM) was firstly peeled off carefully from a fresh eggshell and cleaned 10 times with deionized water to remove residual egg white and then dried at room temperature. The clean ESM was cut into small pieces and soaked into 0.1 mol L^{-1} manganese acetate solution with a certain proportion (0.5 g to 100 mL). After 12 hours, the adsorbed ESM pieces were taken out and washed 5 times with deionized water and placed onto a watch glass to dry. At last, a Chinese Brush was dipped in 0.1 mol L^{-1} NaOH solution for 20 seconds. NaOH solution as ink was brushed evenly on the adsorbed ESM. Five minutes later, the color change of the membrane from white to light brown indicated that the MnO_2 SMPs were synthesized successfully. The MnO_2/ESM piece was washed and dried to preserve for characterization and practical use.

2. 3. Treatment of Methylene Blue Wastewater

15 mg MnO_2/ESM materials and equal amounts of ESM, as a control experiment, were placed in the 4 mL MB solution with the concentration of 8 mg L^{-1} under stirring. After 35 min, materials and ESM were taken out to stop the adsorption. The UV-vis spectra of MB solutions after adsorption were recorded immediately at room temperature. All of the absorption intensity of MB measurement was set at wavelength 664 nm. The removal efficiency (R, %) and adsorption capacity (q_e, mg g^{-1}) were calculated using the equations below:

$$R = \frac{C_0 - C_e}{C_0} \times 100\% \quad (1)$$

$$q_e = \frac{(C_0 - C_e) \times V}{W} \quad (2)$$

where C_0 and C_e (mg L^{-1}) stand for the initial and final concentrations of MB in the treatment solutions, respectively, V is the volume of the mixture solution (L), and W is the mass of adsorbent used (g).

3. Results and Discussion

3. 1. Synthesis Mechanism

Scheme 1 displays the schematic diagram of the synthesis process of submicro-structured MnO_2 on ESM using Chinese Brush. As reported, eggshell membrane is composed of fibrous proteins with different kinds of acidic/basic amino acid residues like –OH, –COOH, $–NH_2$, –SH, etc on the surface. When ESM pieces were soaked into the manganese acetate solution, Mn^{2+} showed a trend (from lone electron pair of heteroatom and unoccupied orbital in Mn atom) to adsorb onto the "active site" on the ESM, which resulted in a uniformly dispersive distribution of Mn^{2+} on the fibrous proteins. After washing and drying

at the room temperature, Chinese Brush with NaOH solution was brushed on the adsorbed ESM. This step caused a reaction in situ between Mn^{2+} and OH^- around these "active site" and as a result MnO_2 were obtained after 5 min.[57] Owing to the uniformly dispersion of Mn^{2+} on the membrane, MnO_2 particles were generated and grew along with the fibrous proteins to form a biomimetic material.

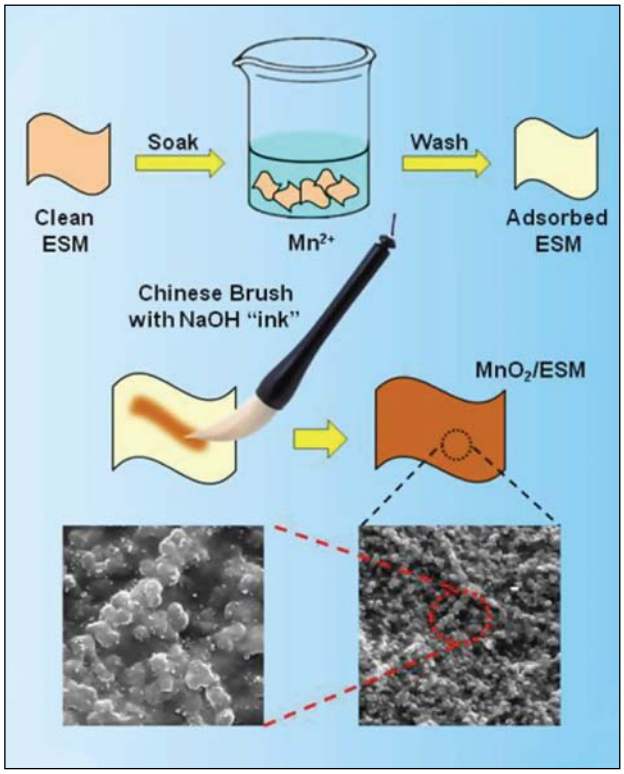

Scheme 1. The schematic diagram of the synthesis process of MnO_2 SMPs on ESM using Chinese Brush.

3. 2. Characterization of MnO_2 SMPs

3. 2. 1. Scanning Electron Microscopy

Morphologies of ESM before and after MnO_2 preparation were investigated for comparison. Figure 1a displays the scanning electron microscopy (SEM) images of ESM, in which multilayer and overlapping fibrous proteins are observed. After the reaction with MnO_2, by contrast, plenty of spherical particles array densely on the adsorbed membrane (Figure 1b and Figure S1a). Interestingly, particles arraying along with the original fiber-like protein is observed, and it is more obvious and straightforward in SEM image with smaller amplification factor (Figure S1a). To measure the particle size of synthesized material, a Nano Particle Analyzer testing was carried out. The results are shown in Figure S1b. And an average diameter of ~710 nm is obtained, which is a good consistency with the microstructured biotemplate.

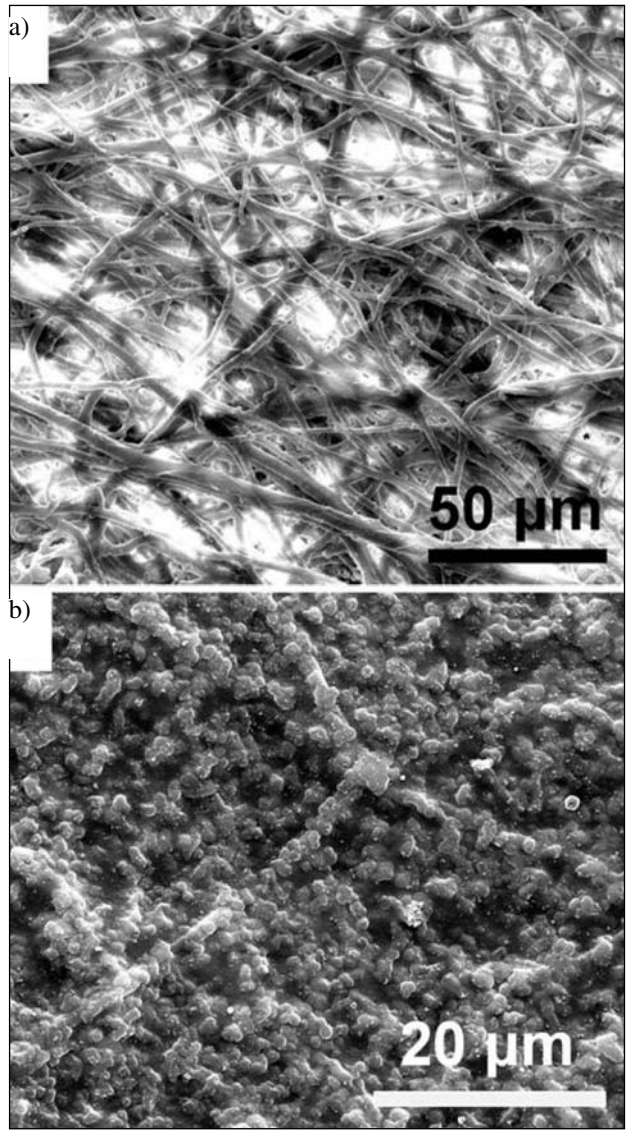

Figure 1. SEM images of (a) ESM and (b) MnO_2 SMPs. Scale bar were 50 μm and 20 μm, respectively.

3. 2. 2. UV-Vis Spectroscopy and X-ray Photoelectron Spectroscopy

The UV-Vis spectrum of as-prepared MnO_2 SMPs is shown in Figure S2. A single absorption peak at 360 nm is found. To investigate the surface composition and elemental analysis for the resultant MnO_2 SMPs, the X-ray photoelectron spectroscopy (XPS) was carried out. In the full scan spectrum (Figure S3), it shows that the synthesized material is composed of elements Mn 2p, O 1s, C 1s and N 1s. The elements C 1s, N 1s and partial O 1s come from proteins in ESM. To examine the details, XPS spectra of Mn 2p and O 1s were measured. As shown in Mn 2p spectrum (Figure 2a), two peaks are observed at 654.2 and 642.4 eV, which can be assigned to Mn $2p_{1/2}$ and Mn $2p_{3/2}$, respectively. Meanwhile, the O 1s spectrum (Figure 2b) can be resolved into three peaks. The strongest peak at

531.4 eV corresponds to the Mn–O–H, the other two small peaks (532.2 eV and 530.0 eV) adjacent reveal the existence of H–O–H and Mn–O–Mn, respectively. As a consequence, the aforementioned findings confirm that the as-prepared submicroparticles are MnO_2.

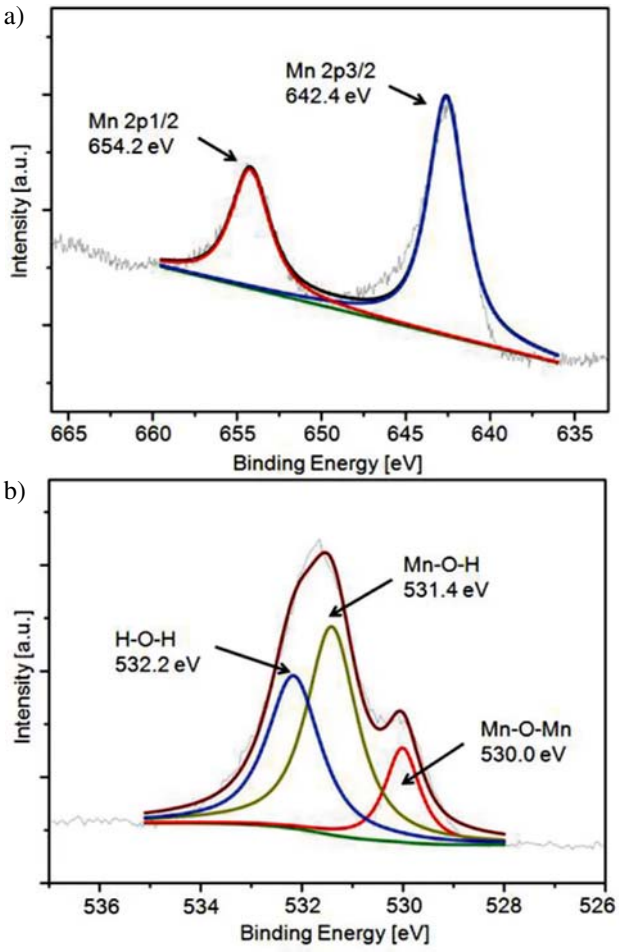

Figure 2. (a) Mn2p and (b) O1s XPS spectra of as-prepared MnO_2 SMPs.

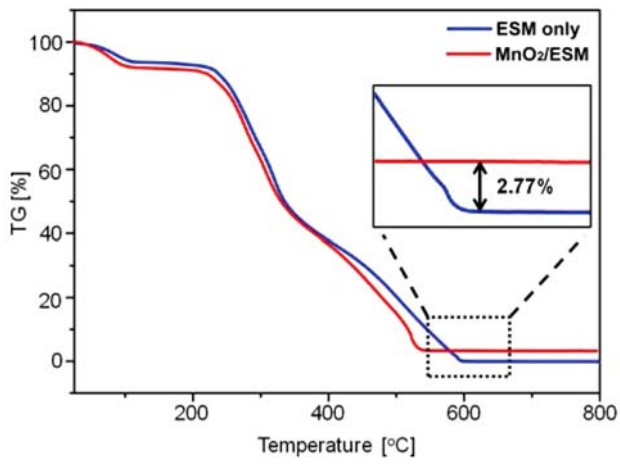

Figure 3. The TG curves of ESM and as-prepared MnO_2 SMPs.

3. 2. 3. Thermogravimetry Analysis

Furthermore, a thermogravimetry (TG) analysis was carried out to illustrate the content of the composite (Figure 3). Blue and red curves indicate the mass changes of ESM only and synthesized MnO_2/ESM material, respectively. It can be seen that ESM, as a kind of protein, is burnt out at about 600 °C and the quality is almost zero (blue curve in Figure 3). To study the relative amount of MnO_2 SMPs coated on ESM, dotted portion in Figure 3 is zoomed in. It is vividly shown that the curves remain unchanged with the temperature rising afterwards. However, the horizontal part of MnO_2/ESM is obviously higher than that of ESM only, which is attributed to the inorganic material existence. The difference of two horizontal curves stands for the relative amount of MnO_2 SMPs in ESM, which is calculated to be 2.77%.

3. 3. Methylene Blue Wastewater Treatment

The detailed characterization and measurement demonstrate that the synthesized material is ESM coated

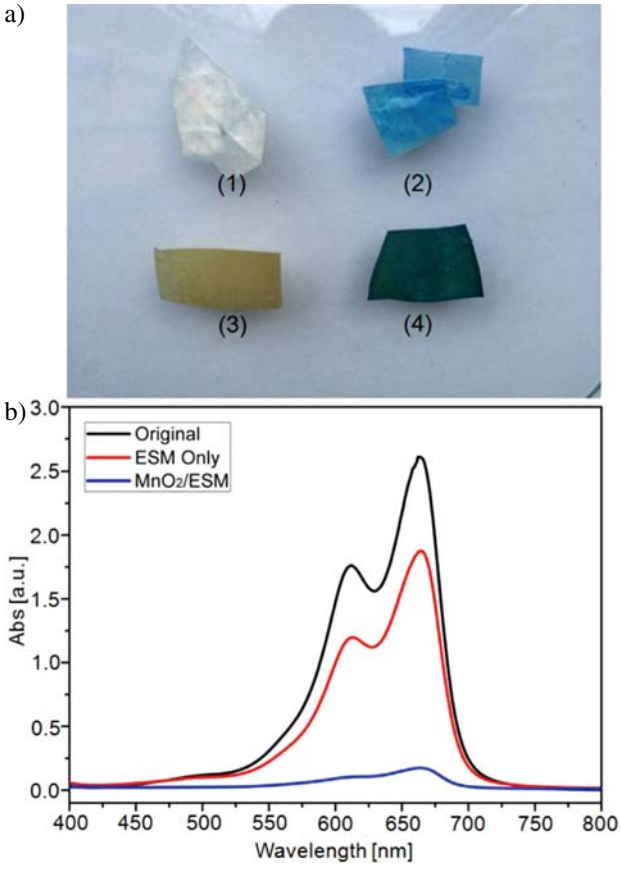

Figure 4. (a) Photographs of ESM and MnO_2/ESM before and after adsorption of MB [(1) ESM only; (2) ESM only after adsorption of MB; (3) MnO_2/ESM SMPs; (4) MnO_2/ESM after adsorption of MB.]. (b) The UV-vis absorption spectra of MB before and after adsorption by ESM only and MnO_2/ESM.

MnO_2 SMPs (MnO_2/ESM). Owing to the handy operation of "put in" and "take out", these materials were further applied to removal of MB. Figure 4a displays the photographs of ESM and MnO_2/ESM before and after adsorption of MB. Two sets of contrastive pictures show that ESM itself is capable of adsorbing for MB. Light pink ESM (1) turns into blue (2) after adsorption of a certain amount of MB. However the color change degree of MnO_2/ESM before and after adsorption is bigger: brown MnO_2/ESM (3) becomes dark green (4). The UV-Vis absorption spectra of MB before and after adsorption by ESM only and MnO_2/ESM are recorded in Figure 4b. It is evidently indicated that the absorption intensity of MB at 664 nm after MnO_2/ESM adsorption is significantly smaller than the one treated with ESM only. Figure S4a exhibits the equation of linear regression of MB solutions, by which the removal efficiencies of ESM and MnO_2/ESM adsorption are calculated in Figure S4b. Inset photographs shows the color change of MB solution before and after adsorption: (5) is original MB solution; (6) and (7) are MB solution after ESM and MnO_2/ESM adsorption, respectively. The color gap between (5) and (7) keeps pace with the removal efficiency of 93% by MnO_2/ESM adsorption.

3. 4. Investigation of Time and pH for Adsorption

Adsorption time for MB by MnO_2/ESM adsorption was investigated by UV-Vis spectroscopy as shown in Figures 5a and S5a. Under different adsorption time the absorption intensity decreases gradually as a function of time and remains the same after 35 min, which represents the whole adsorption process. Figure S5a shows the time dependent removal efficiency curve for MB, it can be seen that the removal efficiency increases rapidly at first 10 min and flats out gradually afterwards. A maximal removal efficiency of 93% is obtained at 35 min. Moreover, Figure S5b demonstrates the effect of pH condition on the adsorption by MnO_2/ESM. It turns out that the removal efficiency is kept in the range of 50%–62% under different pH values. The pH is not a factor to influence within the experimental error. It is worth noting that the removal efficiency under a certain pH condition is not as high as that in the distilled water solution. The additional adsorption for ions, which was used to adjust the acidity of the solution, took charge of this phenomenon. The desorption of MB was performed by placing the adsorbed MnO_2/ESM into deionized water. Figure 5b shows the absorption spectra of MB by adsorption for 35 min and desorption for 24 h. It is seen obviously that the shape and position of absorption peak are the same before and after adsorption, which indicates that the molecule structure of MB keeps unchanged during the removal procedure. Therefore, the removal procedure is an adsorption-desorption equilibrium process.

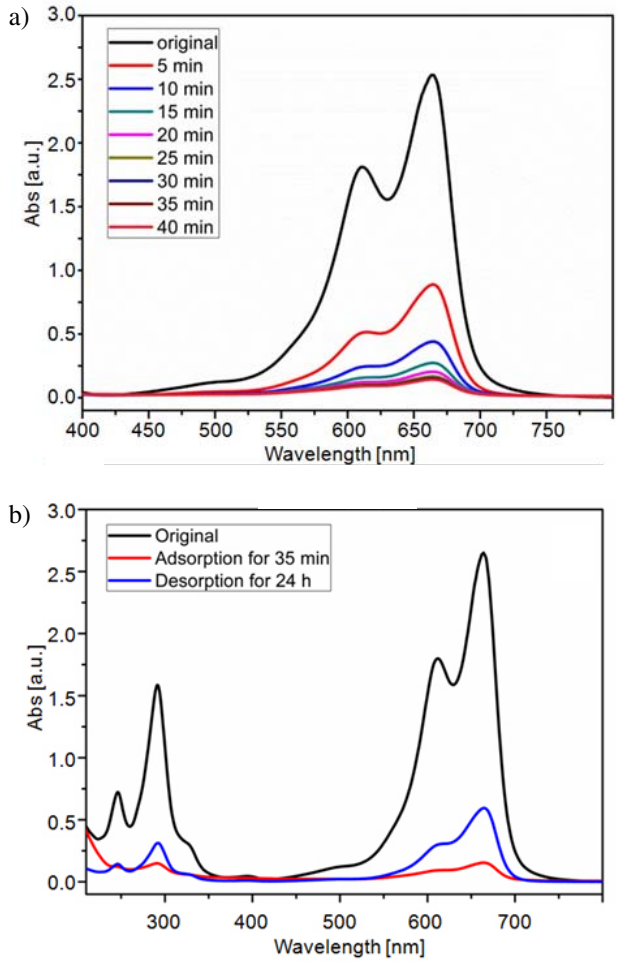

Figure 5. (a) The UV-vis absorption spectra of MB under different time by MnO_2/ESM adsorption. (b) The UV-vis absorption spectra of MB by adsorption for 35 min and desorption for 24 h.

3. 5. Study of Kinetics and Adsorption Isotherm

In order to better understand the adsorption behavior of MB on MnO_2/ESM, the adsorption capacities at different time (q_t) were recorded. As shown in Figure 6a, the adsorption of MB increases gradually with the time prolonged and becomes balanced after 35 min. Based on this, experimental data are calculated and organized in Figure 6b to investigate the adsorption kinetics. Two kinetic models are generally used to evaluate the adsorption,[59] and it can be concluded that the adsorption process of MB on MnO_2/ESM is in accordance with the pseudo-second-order model (correlation coefficient of 0.99508 for pseudo-first-order model and 0.99915 for pseudo-second-order model).

Moreover, the effect of initial MB concentration on equilibrium adsorption capacity (q_e) is shown in Figure 7a, where the adsorption capacity steadily enhances with increasing the initial concentration of MB added. The adsorption behavior of MB on MnO_2/ESM

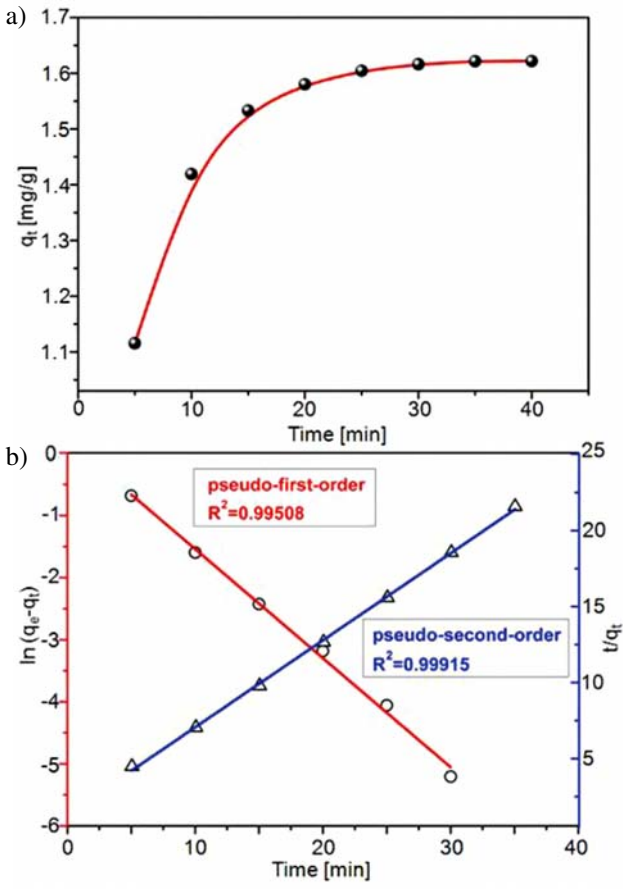

Figure 6. (a) Effect of adsorption time on adsorption capacity of MnO_2/ESM in MB solutions. (b) Pseudo-first-order (red line) and pseudo-second-order (blue line) models for MB adsorption.

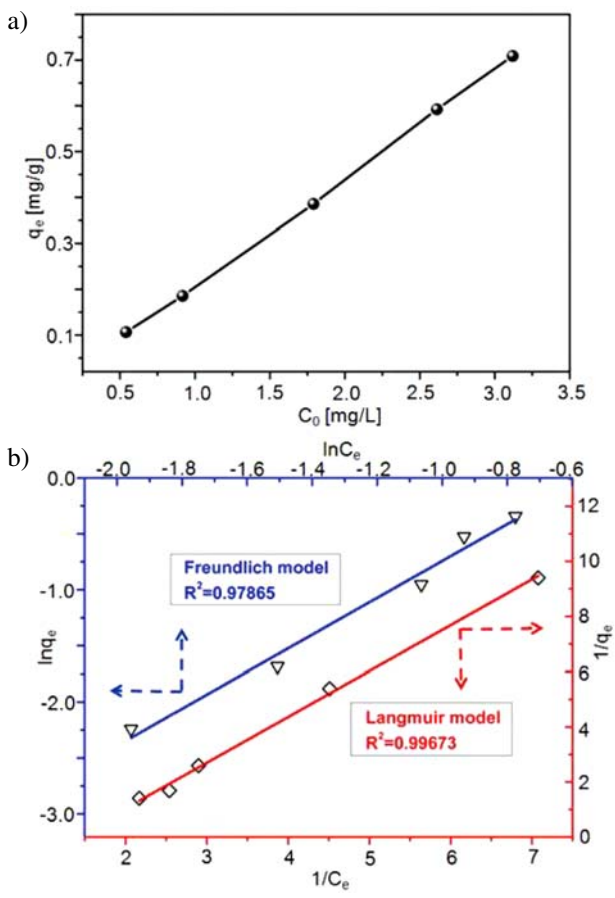

Figure 7. (a) Effect of initial concentrations of MB on equilibrium adsorption capacity of MnO_2/ESM in MB solutions. (b) Langmuir (red line) and Freundlich (blue line) isotherms models for MB adsorption.

was further studied through Langmuir and Freundlich isotherms models (Figure 7b), which were common adsorption isotherms models for evaluating the adsorption process.[59] According to the data calculation and linear fitting, it is concluded that Langmuir model is able to interpret the MB adsorption process better (correlation coefficients are 0.9967 and 0.9787 for Langmuir isotherms and Freundlich isotherms models, respectively).

3. 6. Effect of Hydrogen Peroxide on Removal of MB

The effect of H_2O_2 on the dye MB as a function of time monitored by UV-visible spectra was investigated in Figure S6a. We observed that the presence of H_2O_2 affected the absorbance of dye itself about 5% in 35 min and the shape of the peaks underwent no change. Then the effect of H_2O_2 with various concentrations on the removal efficiency of dye MB decontamination by MnO_2 was examined. The results are showed in Figure S6b. It is straightforward that H_2O_2 decreases the removal efficiency of dye MB by MnO_2.

4. Conclusions

The MnO_2 submicroparticles were prepared through an eggshell membrane based biotemplating method. The size of MnO_2 SMPs kept correspondence with the diameter of the fibrous proteins, which indicated the bio-inspired growth of MnO_2 SMPs. Taking advantages of macro-operability and adsorption performance stemmed from both protein membrane and hydroxyl on the surface of MnO_2 in the aqueous solution, the ESM coated MnO_2 SMPs was applied to the MB wastewater treatment. The adsorption process followed the pseudo-second-order kinetic model and Langmuir isotherms model, and the removal efficiency could reach up to 93% under room temperature without pH adjustment. This simple, green and interesting approach gives a facile concept of metal oxide materials synthesis, which is considered of great potential applications in wastewater treatment area.

5. Acknowledgements

This work was supported by the Key Science Fund Project of Taiyuan Institute of Technology (2015LZ01)

and the Program for the (Reserved) Discipline Leaders of Taiyuan Institute of Technology. We thank Institute of Coal Chemistry, Chinese Academy of Science for the material characterization.

6. References

1. A. Kumar and V. Kumar, *Chem. Rev.* **2014**, *14*, 7044–7078. https://doi.org/10.1021/cr4007285
2. W. Zhang, D. Zhang, T. Fan, J. Ding, J. Gu, Q. Guo and H. Ogawa, *Mater. Sci. Eng. C* **2009**, *29*, 92–96. https://doi.org/10.1016/j.msec.2008.05.013
3. Y. Kim, *Biomacromolecules* **2003**, *4*, 908–913. https://doi.org/10.1021/bm0257558
4. C. R. Rambo and H. Sieber, *Adv. Mater.* **2005**, *17*, 1088–1091. https://doi.org/10.1002/adma.200401049
5. M. L. Chacón-Patiño, C. Blanco-Tirado, J. P. Hinsetroza and M. Y. Combariza, *Green Chem.* **2013**, *15*, 2920–2928. https://doi.org/10.1039/c3gc40911b
6. S. R. Hall, H. Bolger and S. Mann, *Chem. Commun.* **2003**, 2784–2785. https://doi.org/10.1039/b309877j
7. I. W. -S. Lin, C. -N. Lok and C. -M. Che, *Chem. Sci.* **2014**, *5*, 3144–3150. https://doi.org/10.1039/c4sc00138a
8. R. Ramanathan, A. P. O'Mullane, R. Y. Parikh, P. M. Smooker, S. K. Bhargava and V. Bansal, *Langmuir* **2011**, *27*, 714–719. https://doi.org/10.1021/la1036162
9. S. K. Das, J. Liang, M. Schmidt, F. Laffir and E. Marsili, *ACS Nano* **2012**, *6*, 6165–6173. https://doi.org/10.1021/nn301502s
10. L. M. Rösken, S. Körsten, C. B. Fischer, A. Schönleber, S. van Smaalen, S. Geimer and S. Wehner, *J. Nanopart. Res.* **2014**, *16*, 2370. https://doi.org/10.1007/s11051-014-2370-x
11. C. Yang, C. -H. Choi, C.-S. Lee and H. Yi, *ACS Nano* **2013**, *7*, 5032–5044. https://doi.org/10.1021/nn4005582
12. M. G. Warner and J. E. Hutchison, *Nat. Mater.* **2003**, *2*, 272–277. https://doi.org/10.1038/nmat853
13. S. -Y. Pu, A. Zinchenko, L. -L. Qin, C. -W. Ye, M. Xu and S. Murata, *Mater. Lett.* **2014**, *130*, 168–171. https://doi.org/10.1016/j.matlet.2014.05.066
14. W. -Y. Chen, G. -Y, Lan and H. -T. Chang, *Anal. Chem.* **2011**, *83*, 9450–9455. https://doi.org/10.1021/ac202162u
15. L. A. Gugliotti, D. L. Feldheim and B. E. Eaton, *Science* **2004**, *304*, 850. https://doi.org/10.1126/science.1095678
16. J. Xie, Y. Zheng and J. Y. Ying, *J. Am. Chem. Soc.* **2009**, *131*, 888–889. https://doi.org/10.1021/ja806804u
17. J. M. Galloway and S. S. Staniland, *J. Mater. Chem.* **2012**, *22*, 12423–12434. https://doi.org/10.1039/c2jm31620j
18. R. M. Choueiri, A. Klinkova, H. Thérien-Aubin, M. Rubinstein and E, Kumacheva, *J. Am. Chem. Soc.* **2013**, 1*35*, 10262–10265. https://doi.org/10.1021/ja404341r
19. L. Au, B. Lim, P. Colletti, Y. -S. Jun and Y. Xia, *Chem. -Asian J.* **2010**, *5*, 123–129. https://doi.org/10.1002/asia.200900468
20. R. Murugan and S. Ramakrishna, *Biomaterials* **2004**, *25*, 3829. https://doi.org/10.1016/j.biomaterials.2003.10.016
21. M. B. Dickerson, K. H. Sandhage and R. R. Naik, *Chem. Rev.* **2008**, *108*, 4935–3978. https://doi.org/10.1021/cr8002328
22. R. K. Watt, O. D. Petrucci and T. Smith, *Cata. Sci. Technol.* **2013**, *3*, 3103–3110. https://doi.org/10.1039/c3cy00536d
23. C. Sun, H. Yang, Y. Yuan, X. Tian, L. Wang, Y. Guo, L. Xu, J. Lei, N. Gao and G. J. Anderson, *J. Am. Chem. Soc.* **2011**, *133*, 8617–8624. https://doi.org/10.1021/ja200746p
24. J. Fan, J. –J. Yin, B. Ning, X. Wu, Y. Hu, M. Ferrari, G. J. Anderson, J. Wei, Y. Zhao and G. Nie, *Biomaterials* **2011**, *32*, 1611–1618. https://doi.org/10.1016/j.biomaterials.2010.11.004
25. M. Suzuki, M. Abe, T. Ueno, S. Abe, T. Goto, Y. Toda, T. Akita, Y. Yamada and Y. Watanabe, *Chem. Commun.* **2009**, 4871–4873. https://doi.org/10.1039/b908742g
26. M. Li, D. -P. Yang, X. Wang, J. Lu and D. Cui, *Nanoscale Res. Lett.* **2013**, *8*, 1–5. https://doi.org/10.1186/1556-276X-8-1
27. H. Cao, D. -P. Yang, D. Ye, X. Zhang, X. Fang, S. Zhang, B. Liu and J. Kong, *Biosens. Bioelectron.* **2015**, *68*, 329–335. https://doi.org/10.1016/j.bios.2015.01.003
28. C. Hu, D. -P. Yang, Z. Wang, P. Huang, X. Wang, D. Chen, D. Cui, M. Yang and N. Jia, *Biosens. Bioelectron.* **2013**, *41*, 656–662. https://doi.org/10.1016/j.bios.2012.09.035
29. C. Hu, D. -P. Yang, F. Zhu, F. Jiang, S. Shen and J. Zhang, *ACS Appl. Mater. Interfaces* **2014**, *6*, 4170–4178. https://doi.org/10.1021/am405841k
30. C. Hou, D. Yang, B. Liang and A. Liu, *Anal. Chem.* **2014**, *86*, 6057–6063. https://doi.org/10.1021/ac501203n
31. Q. Liu, X. Jiang, S. Gao, H. Xu and L. Sun, *Mater. Lett.* **2014**, *128*, 322–324. https://doi.org/10.1016/j.matlet.2014.04.108
32. E. I. Alarcon, K. Udekwu, M. Skog, N. L. Pacioni, K. G. Stamplecoskie, M. González-Béjar, N. Polisetti, A. Wickham, A. Richter-Dahlfors and M. Griffith, *Biomaterials* **2012**, *33*, 4947–4956. https://doi.org/10.1016/j.biomaterials.2012.03.033
33. X. Huang, H. Wu, S. Pu, W. Zhang, X. Liao and B. Shi, *Green Chem.* **2011**, *13*, 950–957. https://doi.org/10.1039/c0gc00724b
34. P. Zhang, J. Lan, Y. Wang and C. Z. Huang, *Biomaterials* **2015**, *36*, 26–32. https://doi.org/10.1016/j.biomaterials.2014.08.026
35. M. Baláž, *Acta. Biomater.* **2014**, *10*, 3827–3843. https://doi.org/10.1016/j.actbio.2014.03.020
36. N. Li, L. Niu, Y. Qi, C. K. Y. Yiu, H. Ryou, D. D. Arola, J. Chen, D. H. Pashley, F. R. Tay, *Biomaterials* **2011**, *32*, 8743–8752. https://doi.org/10.1016/j.biomaterials.2011.08.007
37. P. S. Devi, S. Banerjee, S. R. Chowdhury and G. S. Kumar, *RSC Adv.* **2012**, *2*, 11578.
38. Q. W. Tang, J. H. Wu, Z. Y. Tang, Y. Li, J. M. Lin and M. L. Huang, *J. Mater. Chem.* **2011**, *21*, 13354–13364. https://doi.org/10.1039/c1jm11857a
39. Q. W. Tang, Z. Y. Tang, J. H. Wu, J. M. Lin and M. L. Huang, *RSC Adv.* **2011**, *1*, 1453–1456.

40. M. Liang, R. Su, W. Qi, Y. Yu, L. Wang and Z. He, *J. Mater. Sci.* **2014**, *49*, 1639–1947. https://doi.org/10.1007/s10853-013-7847-y
41. H. Su, J. Xu, J. J. Chen, W. J. Moon and D. Zhang, *Appl. Phys. A* **2012**, *106*, 93–97. https://doi.org/10.1007/s00339-011-6561-3
42. H. Su, N. Wang, Q. Dong and D. Zhang, *J. Membr. Sci.* **2006**, *283*, 7–12. https://doi.org/10.1016/j.memsci.2006.07.010
43. R. Camaratta, A. N. C. Lima and M. D. Reyes, *Mater. Res. Bull.* **2013**, *48*, 1569–1574. https://doi.org/10.1016/j.materresbull.2012.12.047
44. Z. Wang, X. Shao, X. Hu, G. Parkinson, K. Xie, D. Dong and C. Z. Li, *Catal. Today* **2014**, *228*, 199–205. https://doi.org/10.1016/j.cattod.2014.01.006
45. M. K. Rath, B. H. Choi, M. J. Ji and K. T. Lee, *Ceram. Int.* **2014**, *40*, 3295–3304. https://doi.org/10.1016/j.ceramint.2013.09.105
46. D. H. Dong, Y. Z. Wu, X. Y. Zhang, J. F. Yao, et al, *J. Mater. Chem.* **2011**, *21*, 1028–1032. https://doi.org/10.1039/C0JM03061A
47. S. M. Pourmortazavi, M. Taghdiri, N. Samimi and M. Rahimi-Nasravadi, *Mater. Lett.* **2014**, *121*, 5–7. https://doi.org/10.1016/j.matlet.2014.01.142
48. J. Cao, Q. H. Mao, L. Shi and Y. T. Qian, *J. Mater. Chem.* **2011**, *21*, 16210–16215. https://doi.org/10.1039/c1jm10862j
49. O. M. Wani, M. Safdar, N. Kinnunen and J. Jänis, *Chem. Eur. J.* **2016**, *22*, 1244–1247. https://doi.org/10.1002/chem.201504474
50. M. Safdar, O. M. Wani and J. Jänis, *ACS Appl. Mater. Interfaces* **2015**, *7*, 25580–25585. https://doi.org/10.1021/acsami.5b08789
51. M. Safdar, T, D, Minh, N. Kinnunen and J. Jänis, *ACS Appl. Mater. Interfaces* **2016**, *8*, 32624–42629. https://doi.org/10.1021/acsami.6b12024
52. L. Wang, J. Chen, X. Feng, W. Zeng, R. Liu, X. Lin, Y. Ma and L. Wang, *RSC Adv.* **2016**, *6*, 65624–65630.
53. X. Chen, G. Wu, T. Lan and W. Chen, *Chem. Commun.* **2014**, *50*, 7157–7159. https://doi.org/10.1039/c4cc01533a
54. X. Feng, Y. Zhang, Y. Li, Z. Huang, S. Chen, Y. Ma, L. Zhang, L. Wang and X. Yan, *Chem. Lett.* **2015**, *44*, 399–401. https://doi.org/10.1246/cl.140971
55. H. Wang, G. Zhao and M. Pumera, *J. Am. Chem. Soc.* **2014**, *136*, 2719–2722. https://doi.org/10.1021/ja411705d
56. H. Tamura, T. Oda, M. Nagayama and R. Furuichi, *J. Electrochem. Soc.* **1989**, *136*, 2782–2786. https://doi.org/10.1149/1.2096286
57. T. Yang, M. L. Chen, X. W. Hu, Z. W. Wang, J. H. Wang and P. K. Dasgupta, *Analyst* **2011**, *136*, 83–89. https://doi.org/10.1039/C0AN00480D
58. X. Liu, Q. Wang, H. H. Zhao, L. C. Zhang, Y. Y. Su and Y. Lv, *Analyst* **2012**, *137*, 4552–4558. https://doi.org/10.1039/c2an35700c
59. L. Y. Hao, H. J. Song, L. C. Zhang, X. Y. Wan, Y. R. Tang and Y. Lv, *J. Colliod Interface Sci.* **2012**, *369*, 381–387. https://doi.org/10.1016/j.jcis.2011.12.023

Povzetek

Kot bio-predlogo (biotemplate) za pripravo submikronskih delcev MnO_2 smo izbrali membrano jajčne lupine in uporabili kitajske čopiče pomočene v raztopino natrijevega hidroksida. Povprečna velikost tako pridobljenih delcev je bila 710 nm in je skladna z mikrostrukturo bio-predloge. Tako smo pripravili učinkovit in priročen absorbent za barvilo metilen modro. Učinkovitost odstranjevanja barvila lahko doseže do 93% v 35 minutah pri sobni temperaturi brez uravnavanje pH, tudi zaradi odličnega adsorpcije iz membrane jajčnih lupin in hidroksilnih skupin na površini kristalov MnO_2 v vodni raztopini. Materiale na membrani lahko ločimo od odpadne vode, izogniti pa se moramo sekundarnemu onesnaženju. S tem zanimivim pristopom k sintezi submikronskih delcev MnO_2 in učinkovitostjo odstranjevanja barvila metilen modro bi se lahko odprla nova pot priprave submikronskih materialov, pomembnih za čiščenje odpadnih voda.